Asian Journal of Chemistry; Vol. 28, No. 7 (2016), 1479-1485

ASIAN JOURNAL OF CHEMISTRY

http://dx.doi.org/10.14233/ajchem.2016.19724

in vitro Evaluation of Zeolite Nanoparticles as Carrier for Delivery of 5-Fluorouracil

HAMDALLAH A. HODALI* and DUA'A M. MARZOUQA

Department of Chemistry, Faculty of Science, The University of Jordan, Amman 11942, Jordan

*Corresponding author: E-mail: h-hodali@ju.edu.jo; hodali19@gmail.com

Received: 11 November 2015; *Accepted*: 6 January 2016; *Published online*: 31 March 2016; AJC-17833

The aim of the work is to evaluate the use of zeolite ZSM-5 nanoparticles for loading and release of 5-fluorouracil. Nanoparticles of zeolite ZSM-5 with different SiO_2/Al_2O_3 ratios have been prepared in both the sodium and acid form. All nanoparticle samples of ZSM-5 were loaded with the model anticancer drug 5-fluorouracil. The loaded and unloaded nanoparticle samples were characterized by XRD, SEM, TGA and FTIR. Loading of ZSM-5 samples was performed in an aqueous saturated solution of 5-fluorouracil. A loading greater than 50 % was achieved for the acid-activated nanopatricles of ZSM-5 with a SiO_2/Al_2O_3 ratio of 30 (in the starting gel). The release experiments were conducted in simulated body fluid at a pH of 7.4 and 37 °C. In general, the acid-activated nanoparticles of ZSM-5 show higher percent loading, lower percent release and smaller first order rate constant than the corresponding non-activated samples.

Keywords: 5-Fluorouracil, ZSM-5, Nanoparticles, Acid-activated, Anticancer drugs.

INTRODUCTION

In view of the great challenges in curing cancer, chemotherapy is still a successful medical protocol in its treatment. An important chemotherapeutic agent that has been widely used is 5-fluorouracil (5-FU). It is a water-soluble pyrimidine analogue that rapidly enters body cells and is converted to the active metabolites that disrupt RNA synthesis and acts as an inhibitor of thymidylate synthase, a nucleotide synthesis enzyme [1]. It is effectively used in the treatment of various kinds of cancers including colon, breast and skin [2-4]. However, 5-fluorouracil is poorly adsorbed and has a short plasma half-life of about 0.5 h [5]. The rapid enzymatic metabolism of 5-fluorouracil requires continuous administration of high doses which lead to high toxicity [6]. Encapsulation of 5-fluorouracil in a delivery system may help in overcoming some drawbacks associated with the use of 5-fluorouracil and may allow for oral administration. In this study, loading of 5-fluorouracil onto zeolite nanoparticles and its release into simulated body fluid (SBF) have been investigated.

Zelites are microporous aluminosilicate materials characterized with their well-ordered pore structures, high specific surface area of excess than 400 m^2/g and their good stability in different media [7,8]. With these attractive properties, zeolites have been used as adsorbents, heterogeneous catalysts and recently as drug delivery systems (DDS's). As a microporous material, zeolites were employed as carriers for small size drugs, such as loading of zeolite Y with sulfonamide antibiotics [9], α-cyano-4-hydroxycinnamic acid [10], doxorubicin [11] and aspirin [12]. Microparticles of the zeolites HY [13], zeolite NaX-FAU [14] and ZSM-5 [15] have been studied as drug delivery system for 5-fluorouracil. Recently there is an increasing interest in using nanoparticles for drug delivery, due to their nano scale particle size and relatively high surface area. In addition, they have certain capabilities such as enhancement of drug distribution, decreasing drug toxicity, improving drug solubility and increasing drug stability. The first nano-based drug (Doxil) was approved in 1995 [16]. In this study, nanoparticles of ZSM-5 with different SiO_2/Al_2O_3 were loaded with 5-fluorouracil and then used to study the release profiles of 5-fluorouracil into simulated body fluid at 37 °C.

EXPERIMENTAL

Tetraethyl orthosilicate (TEOS) (Aldrich Chemicals), aluminum nitrate nonahydrate (Sigma-Aldrich), sodium chloride (BDH), barium chloride dihydrate (Merck), calcium chloride dihydrate (Merck), magnesium chloride hexahydrate (SD fine-Chem Limited), sulfuric acid (98 %, SD fine-Chem Limited), ammonium nitrate (RPL), sodium bicarbonate (Merck), KCl (Riedel de Haën), dipotassium hydrogen trihydrate (Merck), Sodium hydroxide pellets (BDH), sodium sulfate (Merck), hydrochloric acid (35 %, SD fine-Chem Limited), nitric acid (95 %, Merck), 5-fluorouracil (Acros Organics, 99 %) and *tris*(hydroxymethyl)aminomethane (Merck) were used as received.

Preparation of ZSM-5 nanoparticles: Nanoparticles of zeolite ZSM-5 with different molar SiO_2/Al_2O_3 ratios were prepared following a literature procedure [17], with some modifications. In a typical procedure: Tetraethyl orthosilicate (12.50 g) was added to a solution containing tetrapropylammonium hydroxide (12.00 g, 25 m % in water) and deionized water (50.0 mL). The flask containing the mixture was placed in a water bath/shaker at 80 °C for 24 h. A solution of appropriate amount of aluminum nitrate nonahydrate (0.45, 0.75 or 1.50 g), sodium hydroxide (0.24 g) and deionized water (4.00 g) was prepared and added to the mixture. The mixture was then placed in an autoclave lined with Teflon and heated at 170 °C for 24 h, for crystallization. The molar composition of the gel was: $1SiO_2$:nAl_2O_3:0.25TPAH:$0.5Na_2O$:$50H_2O$. The value of n is dependent on the amount of aluminum nitrate nonahydrate used. The product was collected by centrifugation and calcined at 550 °C for 6 h. The ZSM-5 nanoparticles were coded as n-ZSM-5(30), n-ZSM-5(60) and n-ZSM-5(100). The chemical composition of samples was determined using an X-ray fluorescence spectrometer (SHIMADZU model XRF-1800).

Preparation of the acid-activated ZSM-5 nanoparticles: Nanoparticles of the zeolite (sodium form), n-ZSM-5, was acid activated into n-H-ZSM-5 using the following typical procedure: a sample of n-ZSM-5 (1.00 g) was added to a solution of ammonium nitrate (50.0 mL; 2.0 M) and the mixture was placed in a water bath/shaker at 80 °C for 24 h, to obtain the ammonium exchanged zeolite, n-NH_4-ZSM-5. The ammonium form of the zeolite was transformed to the acid form by calcination at 500 °C for 4 h [18]. The acid activated samples were coded as n-H-ZSM-5-(30), n-H-ZSM-5-(60), n-H-ZSM-5-(100).

Characterization of the ZSM-5 nanoparticles: All samples of ZSM-5 (sodium form, acid form and drug-loaded) were characterized by using X-ray powder diffraction (XRD). The XRD spectra were measured using XRD-7000 Shimadzu diffractometer (Cu-K_α radiation source, λ = 1.5418 Å) at a scan rate of 2 °C/min.

Morphologies of ZSM-5 nanoparticles were monitored by SEM using an FEI-FEG INSPEC F50 instrument. Random micrographs of the nanoparticles were taken at different magnification powers. The thermogravimetric data was used to evaluate the loading capacity of the drug-loaded samples. The thermogravimetric curves were recorded at a heating rate of 20 °C per min under nitrogen and in the temperature range, room temperature-1000 °C, using Netzsch Sta 409 PC instrument (NETZSCH-Ger) and a Mettler-Toledeo DSC 823 E instrument. Supporting evidence for the drug loading onto ZSM-5 was also obtained from FTIR-spectrometry. FTIR spectra (4000-400 cm^{-1}, KBr pellets) of the drug, unloaded ZSM-5 and drug-loaded ZSM-5 nanoparticles were recorded using a Thermo Nicolet NEXUS 670 FT-IR spectrometer.

Loading of 5-fluorouracil into ZSM-5 and H-ZSM-5 nanoparticles: 5-Fluorouracil was loaded into samples of nanoparticles of ZSM-5 having different SiO_2/Al_2O_3 molar ratios *via* the following general procedure: A solution of 5-fluorouracil (0.4 g) in water (25.0 mL) was added to a flask containing nanoparticles of ZSM-5 (0.2 g). The mixture was stirred in the dark at room temperature for 24 h. The drug-loaded nanoparticles were separated using high speed centrifuge and then dried under vacuum at 60 °C for 2 h.

Loading capacity measurements: The loading capacities of drug-loaded samples were determined by TGA within the temperature range 25-1000 °C. The loading capacities were also determined by UV-visible absorption spectrophotometer. In this case, a predetermined amount of drug-loaded carrier (0.0150 g) was suspended in deionized water (100 mL) and the mixture was stirred for 24 h at room temperature. The mixture was then filtered and the concentration of 5-fluorouracil was determined by measuring the absorbance at 266 nm using Cary 100 Bio UV-visible spectrophotometer (Varian). The total amount of drug in the carrier was calculated with reference to a calibration curve in deionized water.

***in vitro* Release studies:** The *in vitro* release studies help in evaluating the drug carrier and its suitability for *in vivo* applications. The *in vitro* release of 5-fluorouracil out of the loaded samples was carried out using the dialysis method (dialysis bag diffusion technique). An exactly measured sample (about 0.0500 g) of zeolite loaded with 5-fluorouracil was introduced into a dialysis bag (MWCO = 3500 Da) containing simulated body fluid solution (2 mL; pH = 7.4). The sealed dialysis bag was immersed in a flask containing 198 mL simulated body fluid (SBF). The flask was covered and placed in a shaking water bath at 37 °C and at constant shaking rate of about 50 shakings per min. At predetermined time intervals (0.083, 0.25, 0.50, 1.0, 2.0, 3.0, 4.0, 5.0, 6.0, 7.0, 8.0, 9.0, 10.0 h), an aliquot (2 mL) was withdrawn from the flask and replaced by an equivalent amount of fresh simulated body fluid, to maintain a constant volume. The release experiments were conducted in triplicate. The concentration of 5-fluorouracil released was determined by measuring the absorbance at 266 nm relative to a calibration curve of 5-fluorouracil in simulated body fluid. The absorbance was measured using a Cary 100 Bio UV-visible spectrophotometer (Varian).The simulated body fluid was prepared following a literature procedure [19] by dissolving the following salts into 1 L solution of deionized water: 8.036 g NaCl, 0.352 g $NaHCO_3$, 0.225 g KCl, 0.230 g $K_2HPO_4 \cdot 3H_2O$, 0.311 g $MgCl_2 \cdot 6H_2O$, 40.0 mL 1M HCl, 0.388 g $CaCl_2 \cdot 2H_2O$, 0.072 g Na_2SO_4 and 6.063 g *tris*(hydroxymethyl)-aminomethane. The pH was adjusted to 7.4 by using 1.0 M HCl.

RESULTS AND DISCUSSION

Synthesis and characterization of nanoparticles of ZSM-5 and H-ZSM-5: Nanoparticles of ZSM-5 (sodium form) were prepared with three different SiO_2/Al_2O_3 molar ratios by using a constant amount of tetraethylorthosilicate and changing the mass of aluminum nitrate in the hydrogel (Table-1). As clearly seen in Table-1, the SiO_2/Al_2O_3 molar ratio in the final product is less than that in the precursor gel indicating that not all tetraethylorthosilicate participate in the polymerization process. The produced nanoparticles were separated by centrifugation, washed with deionized water and then calcined at 550 °C to remove the template. Zeolite ZSM-5 nanoparticles were then acid activated into n-H-ZSM-5 *via* a two-step procedure; the first step involves exchange of the sodium ions by ammonium ions to form (n-NH_4-ZSM-5) and then transformation of the ammonium form into the acid form *via* pyrolysis.

TABLE-1
SiO_2 TO Al_2O_3 RATIO BASED ON THE AMOUNT OF ALUMINUM NITRATE NONAHYDRATE AND TETRAETHYLORTHOSILICATE

Sample codes	Mass of $Al(NO_3)_3{\cdot}9H_2O$ (g)	Mass of $(EtO)_4Si$ (g)	SiO_2/Al_2O_3 (molar ratio)
n-ZSM-5-(30)*	1.50	12.5	30 (17)**
n-ZSM-5-(60)	0.75	12.5	60 (41)
n-ZSM-5-(100)	0.45	12.5	100 (75)

*The number in brackets is the molar ratio of SiO_2/Al_2O_3 in the starting gel. **The molar ratio of SiO2/Al2O3 in the final product.

The XRD spectra of n-ZSM-5 with different SiO_2/Al_2O_3 molar ratios appear almost the same and show the characteristic peaks of MFI structure. The XRD spectra of acid-activated samples are also in full agreement with the typical pattern for zeolite ZSM-5 confirming that zeolite ZSM-5 keeps its structure upon acid activation, as shown in the example given in Fig. 1.

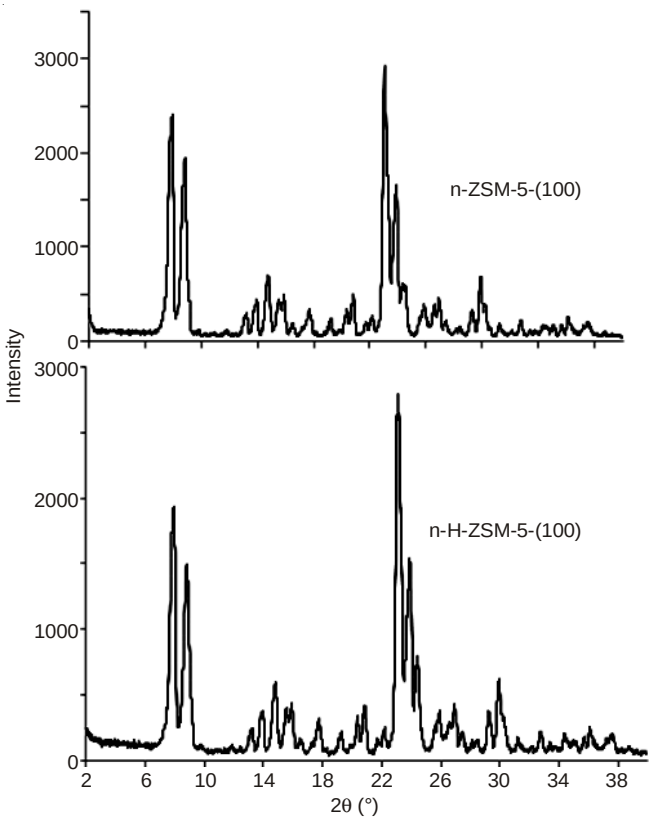

Fig. 1. XRD spectra of n-ZSM-5-(100) and n-H-ZSM-5-(100)

The formation of zeolite nanoparticles was confirmed by scanning electron microscopy. Estimates of the particle sizes of n-ZSM-5 and n-H-ZSM-5 and their morphologies were obtained through SEM micrographs. The particles have hexagonal prismatic shapes with particle size distributions in the range of 300-400 nm. Fig. 2 shows the micrographs of n-ZSM-5-(60) and n-H-ZSM-5-(60).

Loading of 5-fluorouracil onto n-ZSM-5 and n-H-ZSM-5: 5-Flourouracil is relatively a small molecule with approximate dimensions of 4.9 × 5.3 Å. Attempts to use mesoporous materials with large pores for loading of small size drug molecules result in low percent loading. Accordingly and in order to increase the

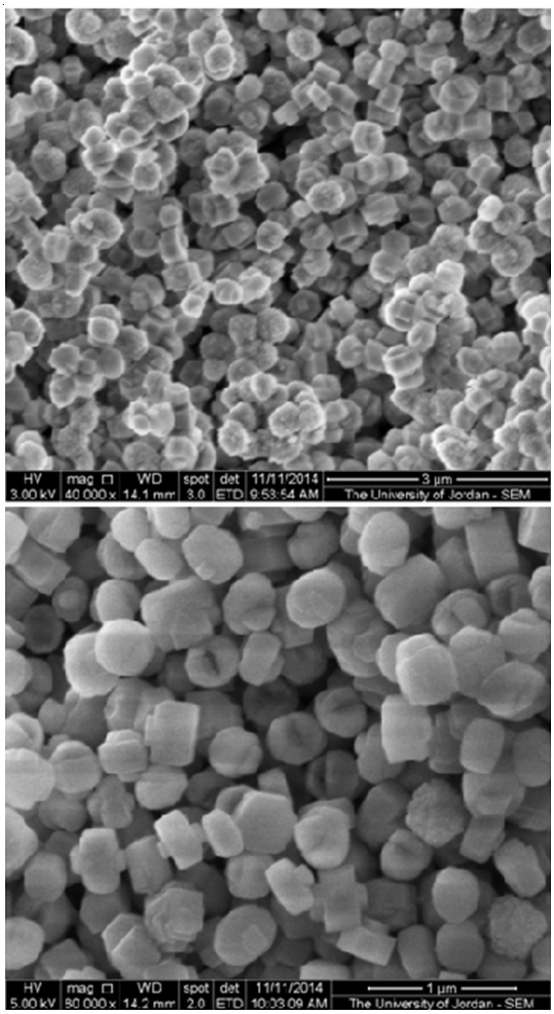

Fig. 2. SEM micrograph of (a) n-ZSM-5-(60) and (b) n-H-ZSM-5-(60)

drug loading capacity, the micro-porous zeolite ZSM-5 was chosen. 5-Fluorouracil was loaded onto samples of n-ZSM-5 and n-H-ZSM-5 with different SiO_2/Al_2O_3 molar ratios by the impregnation method. The highest percent loading was obtained using an aqueous medium of 0.40 mg of 5-fluorouracil and 0.20 g of the zeolite carrier in 25.00 mL DI water with stirring for a period of 24 h at room temperature. Loading of the drug onto the ZSM-5 was confirmed by FTIR-spectrometry and XRD spectra. Comparison of the FTIR spectra of n-ZSM-5, 5-fluorouracil and loaded n-ZSM-5, in the region 2000-400 cm^{-1} (Fig. 3), confirms the presence of the drug in the loaded zeolite. The band at 1770 cm^{-1}, that does not appear in the spectrum of unloaded zeolites, appears as a strong band in the spectrum of free 5-fluorouracil and as a weak band in the spectra of loaded samples of n-ZSM-5 and n-H-ZSM-5. The substantial decrease in the intensity of drug stretching vibrations is characteristic of compounds confined in the pores of porous materials [13,20].

The presence of 5-fluorouracil in the pores of ZSM-5 nanoparticles was also detected by XRD. The 5-fluorouracil characteristic peak at 2θ = 29° appears in the XRD spectrum of drug-loaded n-ZSM-5-(100) (Fig. 4). Although the appearance of this peak confirms drug loading, it also suggests that loading is accompanied with crystallization of 5-fluorouracil in the carrier pores.

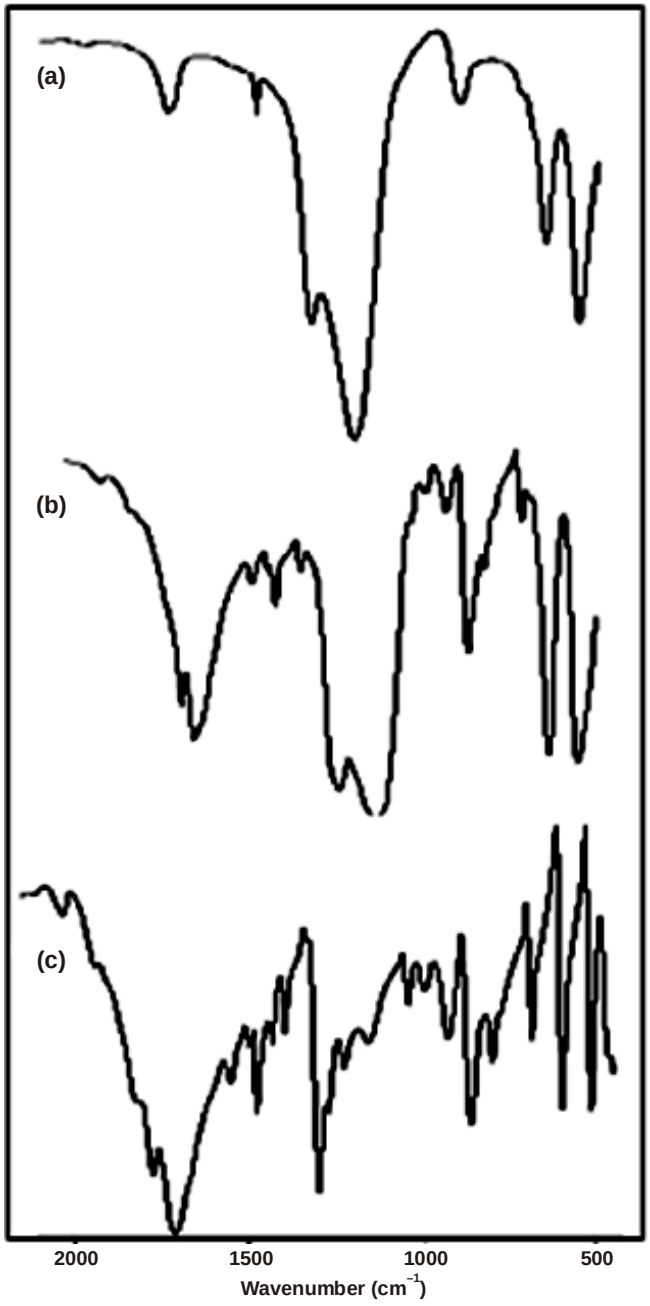

Fig. 3. FTIR spectra of (a) n-ZSM-5-(60), unloaded, (b) n-ZSM-5-(60) loaded with 5-fluorouracil, (c) Free 5-fluorouracil

The loading capacity of the drug-loaded nanoparticles was determined by thermal gravimetric analysis and UV-visible spectrometry. Examples of the thermogravimetric curves (for n-ZSM-5(30) and n-H-ZSM-5-(30)) are shown in Fig. 5. The loading capacity was also determined by UV-visible spectrophotometer, using the following equation:

$$\text{Loading } (\%) = \frac{\text{Mass of drug loaded into carrier}}{\text{Mass of loaded carrier}} \times 100$$

The calculated values of percent loading obtained from TGA measurements and those obtained by UV-visible spectrophotometer are presented in Table-2.

Table-2 reveals two important trends. First, the percent loading of 5-fluorouracil into the nanoparticles of acid-activated forms of ZSM-5 are higher than the corresponding non-activated

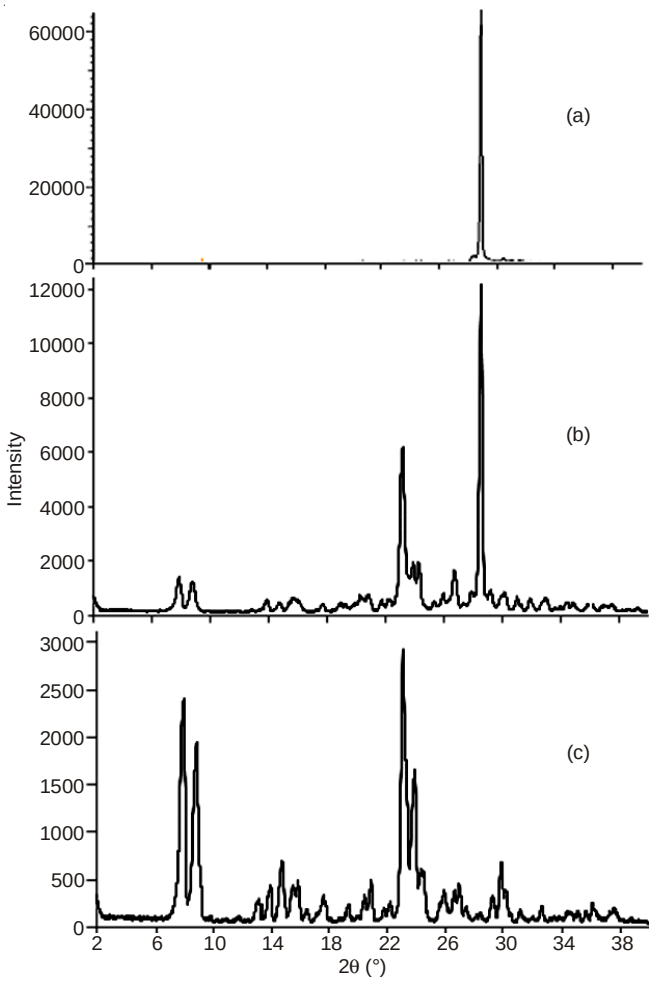

Fig. 4. XRD spectra of (a) 5-fluorouracil, (b) n-ZSM-5-(100) loaded with 5-fluorouracil and (c) unloaded n-ZSM-5-(100)

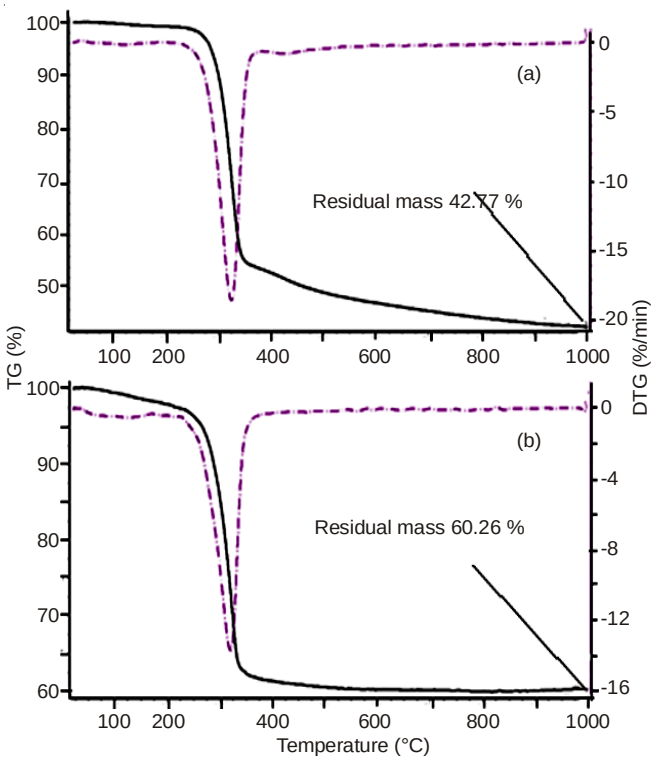

Fig. 5. Thermogravimetric curves of drug-loaded nanoparticles: (a) n-ZSM-5(30) and (b) n-H-ZSM-5-(30)

TABLE-2
PERCENTAGE LOADING OF 5-FLUOROURACIL INTO n-ZSM-5 AND n-H-ZSM-5 WITH DIFFERENT SiO_2/Al_2O_3 MOLAR RATIO

ZSM-5 samples	UV-visible measurement (%)	TGA measurement (%)
n-ZSM-5-(30)	33.2	34.9
n-H-ZSM-5-(30)	52.4	54.9
n-ZSM-5-(60)	30.1	35.7
n-H-ZSM-5-(60)	39.7	42.3
n-ZSM-5-(100)	29.5	30.8
n-H-ZSM-5-(100)	30.3	25.2

forms, with the difference is more pronounced in case of ZSM-5 samples with the lowest SiO_2/Al_2O_3 ratio. Second, it has been observed that percent loading increases with decreasing the SiO_2/Al_2O_3 ratio, whether the sample is acid-activated or non-activated. This could be attributed to increase of zeolite framework polarity with increasing aluminum content. Accordingly, the highest percent loading was observed for acid-activated ZSM-5 nanoparticles with SiO_2/Al_2O_3 ratio of 30, which is about twice the percent loading of non-activated ZSM-5 nanoparticles with SiO_2/Al_2O_3 ratio of 100.

Release of 5-fluorouracil from zeolite ZSM-5: The release of 5-fluorouracil into simulated body fluid at 37 °C and a pH = 7.4 has been conducted using dialysis bags with MWCO of 3500 Da. In these experiments the effect of acid activation and SiO_2/Al_2O_3 ratio on the release of 5-fluorouracil from all ZSM-5 nanoparticles (n-ZSM-5-(30), (n-H-ZSM-5-(30), n-ZSM-5-(60), n-H-ZSM-5-(60), n-ZSM-5-(100), n-H-ZSM-5-(100)) have been studied. Aliquots from the release medium were withdrawn at regular time intervals and were directly replaced by samples of simulated body fluid at the same temperature, thus keeping the simulated body fluid volume constant. The experiments were conducted in triplicate and the averages were used for data analysis. The absorbance of 5-fluorouracil in the release medium was measured at λ_{max} = 266 nm, using a blank sample for base correction. The measured values were then fitted against a calibration curve determined with pure 5-fluorouracil dissolved in simulated body fluid. The drug release profiles for acid-activated and non-activated n-ZSM-5 are presented in Fig. 6. The concentration of 5-fluorouracil in the release medium was used to determine the mass of 5-fluorouracil (W_t) released at time t. This quantity was corrected for the amount of 5-fluorouracil in the previously withdrawn samples by adding the amount of drug in all withdrawn samples prior to that point. The total quantity of drug released at the end of reaction was designated as W_{max}. The full release profiles were fitted with the first order release model [21]:

$$\frac{W_t}{W_{max}} = 1 - e^{-k_t}$$

where W_t/W_{max} is the fraction of drug released, k is the release rate constant and (t) is the elapsed time. The above relation was used to model the release profiles of water-soluble drugs from nonswelling porous matrices [22]. The calculated first order rate constants were determined by fitting W_t against the sampling time (t).

All release profiles (Fig. 6) show an initial burst rate of 5-fluorouracil with about 50 % in the first 15 min. The strong initial burst could be due to the 3D pore structure of ZSM-5 that allows fast release of the drug, or probably due to the existence of 5-fluorouracil at the opening of the pores. The time for maximum release varies between the different system and ranges between 2-4 h. For example, the release from n-ZSM-5-(30) was complete in 2 h, whereas from H-n-ZSM-5(100) it was complete in 4 h. In general, the percent release from the acid-activated ZSM-5 nanoparticles is lower than the corresponding non-activated form. This could be due to the stronger interaction between 5-fluorouracil and the acid-activated inner surface of zeolite pores.

The kinetic parameters for the release of all systems are shown in Table-3. Analysis of these data indicates two general trends: (a) The first order release rate constant increases with increasing the SiO_2/Al_2O_3 ratio. (b) In all cases, the release rate of the acid-activated systems is slower than the corresponding non-activated systems.

Conclusion

In this study, 5-fluorouracil was successfully loaded onto nanoparticles of acid-activated and non-activated ZSM-5 that were prepared with different SiO_2/Al_2O_3 ratios. Loading was carried out by impregnation method and the loading capacity was evaluated by UV and TGA. In all cases, the loading capacities of the acid-activated ZSM-5 nanoparticles are higher than the corresponding non-activated systems, with n-H-ZSM-5-(30) has the highest loading capacity. On the contrary, values of percent release of the acid-activated ZSM-5 nanoparticles are lower than the corresponding non-activated systems. The release of 5-fluorouracil into simulated body fluid at 37 °C and pH = 7.4 followed exponancial decay behaviour. The study represents an evaluation for the suitability of nanoparticles of acid-activated and non-activated ZSM-5 for drug delivery.

TABLE-3
LOADING AND RELEASE KINETIC DATA PARAMETERS OF 5-FLUOROURACIL FROM n-ZSM-5 AND n-H-ZSM-5 WITH DIFFERENT SiO_2/Al_2O_3 RATIOS. MODELING OF % RELEASE (W_t/W_{max}) WAS CARRIED OUT USING THE FIRST ORDER RELEASE MODEL [$W_t/W_{max} = 1 - e^{-kt}$]

System	Loading data			Release data ($W_t/W_{max} = 1 - e^{-kt}$)		
	m_s (mg)[a]	m_d (mg)[b]	Loading (%)	W_{max} (mg)[c]	Release (%)[d]	k (h^{-1})[e]
n-ZSM-5-(30)	48.8	16.7	34.2	14.3	85.5	7.86
n-H-ZSM-5-(30)	57.3	30.1	52.6	21.9	72.8	4.34
n-ZSM-5-(60)	53.6	16.1	30.1	13.4	83.3	2.91
n-H-ZSM-5-(60)	50.2	19.6	39.7	16.1	82.2	2.69
n-ZSM-5-(100)	50.6	14.9	29.5	14.5	97.4	2.37
n-H-ZSM-5-(100)	50.4	20.0	39.7	16.7	83.8	1.92

[a] m_s = Average mass of the drug-loaded sample; [b] m_d = Average mass of the drug in the loaded sample; [c] W_{max} = Maximum mass of drug released into the simulated body fluid buffer solution; [d]Release (%) = $W_t/m_d \times 100$; [e]k = First order rate constant.

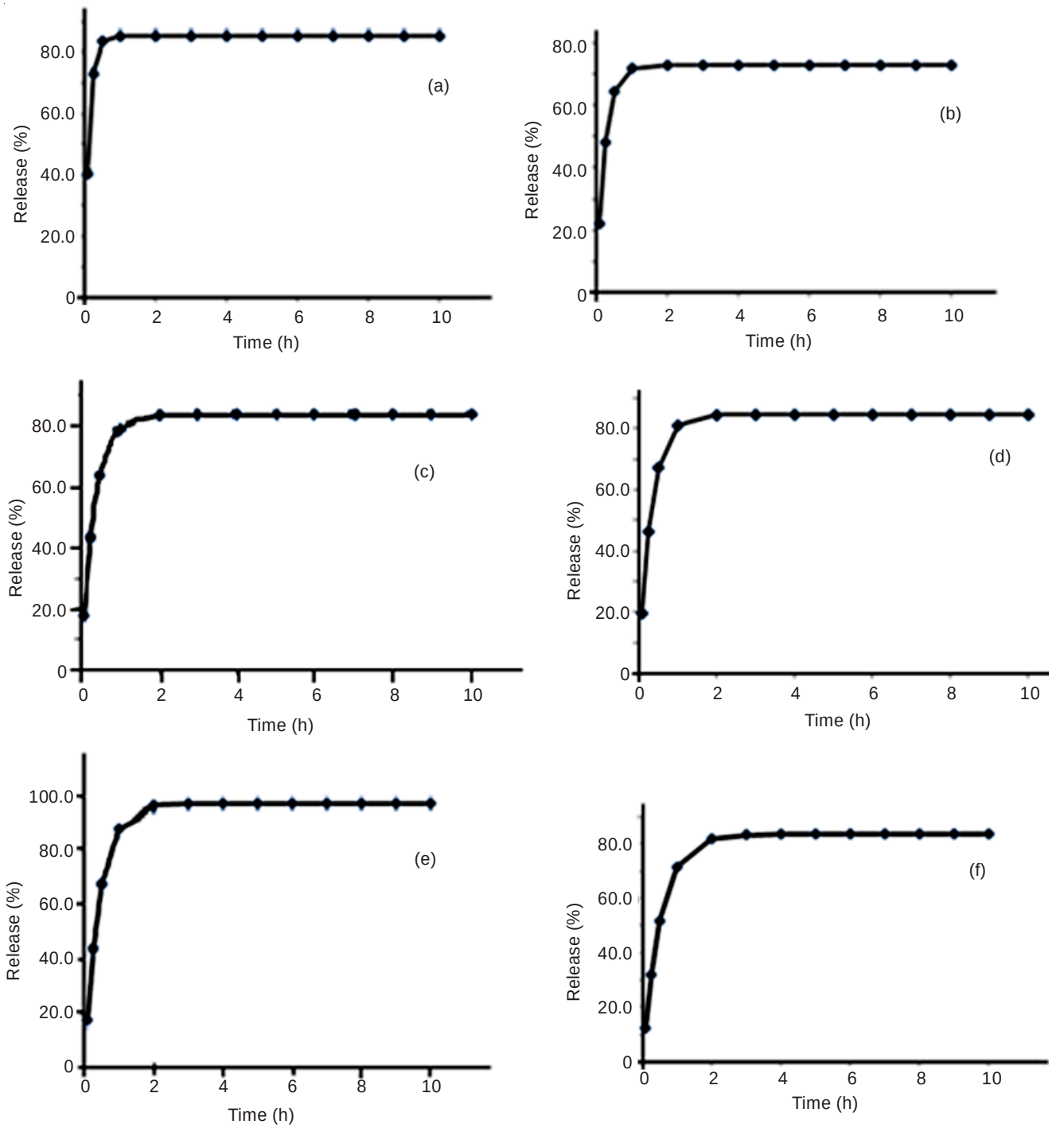

Fig. 6. Release profiles (fitted to first order release kinetics) of 5-fluorouracil from (a) n-ZSM-5-(30), (b) n-H-ZSM-5-(30), (c) n-ZSM-5-(60), (d) n-H-ZSM-5-(60), (e) n-ZSM-5-(100), (f) n-H-ZSM-5-(100)

ACKNOWLEDGEMENTS

The authors are grateful for the financial support from Scientific Research Support Fund (Grant No. Bas/2/02/2012).

REFERENCES

1. D.B. Longley, D.P. Harkin and P.G. Johnston, *Nat. Rev. Cancer*, **3**, 330 (2003).
2. S. Yan, J. Zhu, Z. Wang, J. Yin, Y. Zheng and X. Chen, *Eur. J. Pharm. Biopharm.*, **78**, 336 (2011).
3. T.A. Rich, R.C. Shepard and S.T. Mosley, *J. Clin. Oncol.*, **22**, 2214 (2004).
4. R.B. Diasio and B.E. Harris, *Clin. Pharmacokinet.*, **16**, 215 (1989).
5. R.C. Mundargi, V. Rangaswamy and T.M. Aminabhavi, *Desig. Monomers Polym.*, **13**, 325 (2010).
6. J.L. Arias, *Molecules*, **13**, 2340 (2008).; J.L. Arias, M. Lopez-Viota, A.V. Delgado and M.A. Ruiz, *Colloids Surf. B*, **77**, 111 (2010).
7. M. Danilczuk, K. Dlugopolska, T. Ruman and D. Pogocki, *Mini Rev. Med. Chem.*, **8**, 1407 (2008).
8. D.G. Fatouros, D. Douroumis, V. Nikolakis, S. Ntais, A.M. Moschovi, V. Trivedi, B. Khima, M. Roldo, H. Nazar and P.A. Cox, *J. Mater. Chem.*, **21**, 7789 (2011).
9. I.S. Braschi, S. Blasioli, L. Gigli, C.E. Gessa, A. Alberti and A. Martucci, *J. Hazard. Mater.*, **178**, 218 (2010).
10. N. Vilaca, R. Amorim, O. Martinho, R.M. Reis, F. Baltazar, A.M. Fonseca and I.C. Neves, *J. Mater. Sci.*, **46**, 7511 (2011).

11. M. Arruebo, R. Fernandez-Pacheco, S. Irusta, J. Arbiol, M.R. Ibarra and J. Santamaría, *J. Nanotechnol.*, **17**, 4057 (2006).
12. A. Datt, D. Fields and S.C. Larsen, *J. Phys. Chem. C*, **116**, 21382 (2012).
13. A. Datt, E.A. Burns, N.A. Dhuna and S.C. Larsen, *Micropor. Mesopor. Mater.*, **167**, 182 (2013).
14. M. Spanakis, N. Bouropoulos, D. Theodoropoulos, L. Sygellou, S. Ewart, A.M. Moschovi, A. Siokou, I. Niopas, K. Kachrimanis, V. Nikolakis, P.A. Cox, I.S. Vizirianakis and D.G. Fatouros, *Nanomedicine*, **10**, 197 (2014).
15. R. Al-Thawabeia and H.A. Hodali, *J. Chem.*, Article ID 403597 (2015).
16. Y.C. Barenholz, *J. Control. Rel.*, **160**, 117 (2012).
17. H. Mochizuki, T. Yokoi, H. Imai, R. Watanabe, S. Namba, J.N. Kondo and T. Tatsumi, *Micropor. Mesopor. Mater.*, **145**, 165 (2011).
18. A. Saito and H.C. Foley, *Micropor. Mater.*, **3**, 543 (1995).
19. A. Oyane, H. Kim, T. Furuya, T. Kokubo, T. Miyazaki and T. Nakamura, *J. Biomed. Mater. Res.*, **65A**, 188 (2003).
20. D.M. Marzouqa, M.B. Zughul, M.O. Taha and H.A. Hodali, *J. Porous Mater.*, **19**, 825 (2012).
21. T. Heikkila, J. Salonen, J. Tuura, N. Kumar, T. Salmi, D.Y. Murzin, M.S. Hamdy, G. Mul, L. Laitinen, A.M. Kaukonen, J. Hirvonen and V.P. Lehto, *Drug Deliv.*, **14**, 337 (2007).
22. P. Costa and J.M. Sousa Lobo, *Eur. J. Pharm. Sci.*, **13**, 123 (2001).